N93-18823

A NUMERICAL APPROACH TO CONTROLLER DESIGN FOR THE ACES FACILITY

W. Garth Frazier[1] and R. Dennis Irwin[2]
Department of Electrical and Computer Engineering
Ohio University, Athens, Ohio

INTRODUCTION

In recent years the employment of active control techniques for improving the performance of systems involving highly flexible structures has become a topic of considerable research interest. Most of these systems are quite complicated, using multiple actuators and sensors, and possessing high order models. The majority of analytical controller synthesis procedures capable of handling multivariable systems in a systematic way require considerable insight into the underlying mathematical theory to achieve a successful design. This insight is needed in selecting the proper weighting matrices or weighting functions to cast what is naturally a multiple constraint satisfaction problem into an unconstrained optimization problem. Although designers possessing considerable experience with these techniques have a feel for the proper choice of weights, others may spend a significant amount of time attempting to find an acceptable solution. Another disadvantage of such procedures is that the resulting controller has an order greater than or equal to that of the model used for the design. Of course, the order of these controllers can often be reduced, but again this requires a good understanding of the theory involved.

As an alternative to these synthesis procedures, some numerical techniques have been proposed for achieving design constraints. One technique that appears to be effective is that of Boyd and Barratt (ref. 1). Their approach is to cast the constraints for the design problem into a form such that the optimization is convex over the set of controllers that stabilize a given model of the system. Therefore, the solution is the global optimum and is obtained by standard mathematical programming techniques. Unfortunately, some constraints cannot be cast into a form that is closed loop convex; important ones being open loop controller stability, controller order, and controller structure (e.g., diagonal). A mathematical model of the plant is also required.

A method close in spirit to the technique presented here is that proposed by Newsom and Mukhopadhyay (ref. 2). In their approach the singular value gradients of a return difference operator are used to iteratively change the parameters of a nominal controller in

---

[1]Research Assistant

[2]Associate Professor

order to improve the stability robustness properties of a system. The parameter correction vector at each iteration is chosen to decrease a cumulative measure (sum of squares) of all constraint violations. The disadvantage of this correction vector is that while the cumulative measure may improve, the worst violation is not guaranteed to improve. Recently, Mukhopadhyay (ref. 3) has extended the approach to incorporate other constraints, although a cumulative measure is still employed to monitor each constraint's improvement.

The algorithm employed here for synthesizing a controller for the Active Control Technique Evaluation for Spacecraft (ACES) facility simultaneously includes performance constraints and stability robustness constraints. It also has the advantage that the worst constraint violations are improved at each iteration as long as the constraints are locally feasible in the parameter space. The algorithm can use data generated from a system model or, more importantly, data derived directly from the open loop plant.

SYMBOLS AND ABBREVIATIONS

I	= identity matrix
C	= set of complex numbers
R	= set of real numbers
$Re[\cdot]$	= real part of a complex quantity
$[\cdot]^H$	= complex-conjugate matrix transpose
$[\cdot]^T$	= matrix transpose
$C^{n\times m}$	= set of complex-valued $n \times m$ matrices
$R^{n\times m}$	= set of real-valued $n \times m$ matrices
$\sigma_k[\cdot]$	= k^{th} largest singular value of a matrix
$\partial f/\partial[\cdot]$	= a matrix with (i,j) entry equal to $\partial f/\partial[\cdot]_{ij}$
$\|\cdot\|$	= Euclidean norm of a vector

ALGORITHM DESCRIPTION

Let

$$\Omega = \{\omega_j: j = 1,2,\ldots,N_\omega\} \tag{1}$$

be a set of frequencies at which the frequency response data of the plant is available. Let

$$p = \begin{bmatrix} p_1 & p_2 & \cdots & p_{N_p} \end{bmatrix}^T \tag{2}$$

denote a vector of controller parameters upon which the frequency dependent functions

$$f_i(p):\Omega \rightarrow R, \quad i = 1,2,\ldots,N_c, \tag{3}$$

depend. Define the design constraints by

$$f_i(\omega_j;p) \geq c_i(\omega_j), \quad \forall\ \omega_j \in \Omega, \quad i = 1,2,\ldots,N_c, \tag{4}$$

where each $c_k:\Omega \rightarrow R$ is defined according to the desired shape of f_k. Now define the set of violations at the k^{th} iteration by

$$S_k = \{(i,j):\ f_i(\omega_j;p_k) \leq c_i(\omega_j),\ i = 1,2,\ldots,N_c,\ j = 1,2,\ldots,N_\omega\}. \tag{5}$$

and let $h_{ij}(p_k) = f_i(\omega_j;p_k)$ if $(i,j) \in S_k$. Let N_t be the total number of elements in S_k. It follows that if the partial derivative of f_i with respect to p exists that

$$g_{ij}(p_k) = \left[\frac{\partial h_{ij}}{\partial p_1}(p_k)\ \frac{\partial h_{ij}}{\partial p_2}(p_k)\ \cdots\ \frac{\partial h_{ij}}{\partial p_{N_p}}(p_k)\right]^T. \tag{6}$$

A fundamental result from optimization theory states that to improve a single violation $h_{ij}(p_k)$ a parameter correction vector d_k must be chosen with the property $g_{ij}^T(p_k)d_k > 0$. Since, in general, there are many violations to be improved at any one iteration, d_k should be chosen to satisfy $g_{ij}(p_k)^T d_k > 0$, $\forall\ (i,j) \in S_k$. A sufficient condition for such a direction to exist is that the system

$$J_k^T d_k = w_k \tag{7}$$

be consistent, where J_k is a matrix whose columns are the vectors $g_{ij}(p_k)$ for all $(i,j) \in S_k$, and w_k is a vector such that each entry $w_{kn} > 0$, $n = 1,2,\ldots,N_t$. This is an N_t by N_p system of linear equations. In practice equation 7 is almost always underdetermined because there are usually more free parameters than violations. Hence, there may be many solutions. To obtain the solution having a minimum 2-norm, suppose that J_k has rank r. Then J_k has the singular value expansion (ref. 4),

$$J_k = \sum_{i=1}^{r} \sigma_{ki} u_{ki} v_{ki}^T, \tag{8}$$

where $\sigma_{ki} > 0$, $i = 1,2,\ldots,r$ are the nonzero singular values of J_k, and u_{ki}, v_{ki}, $i = 1,2,\ldots,r$ are the associated left and right singular vectors. If w_k is in the range of J_k^T, then

$$d_k = \sum_{i=1}^{r} \sigma_{ki}^{-1}\left(u_{ki}^T w_k\right) v_{ki}. \tag{9}$$

Although the above development indicates a general procedure for choosing an acceptable correction vector, it does not indicate how to choose the precise entries of w_k for good algorithm performance. Since it is desired to improve all the violations simultaneously,

it seems reasonable to choose w_k such that each of the violations is considered to be equally important. Following the development of Mitchell (ref. 5), if the elements of w_k are chosen such that

$$w_{kn} = \|J_{kn}\|, \tag{10}$$

where J_{kn} is the n^{th} column of J_k which is actually $g_{ij}(p_k)$ for some $(i,j) \in S_k$. Then from equation 7

$$g_{ij}^T(p_k)d_k = \|g_{ij}(p_k)\|, \quad j=1,2,\ldots,N_t. \tag{11}$$

Using the fact that

$$g_{ij}^T(p_k)d_k = \|g_{ij}(p_k)\| \, \|d_k\| \cos\Theta_{ij} = \|g_{ij}(p_k)\|, \tag{12}$$

where Θ_{ij} is the angle between $g_{ij}(p_k)$ and d_k, it is clear that

$$\cos\Theta_{ij} = \|d_k\|^{-1} \quad \forall \ (i,j) \in S_k. \tag{13}$$

Therefore, this choice results in a correction vector that forms an equal angle between itself and each $g_{ij}(p_k)$. The choice of other values for w_k continues to be an area of research interest.

Due to the nonlinearity of the parameter space, it is necessary to determine a satisfactory step length for the correction vector at each iteration. In most iterative algorithms the determination of the step length at each iteration is treated as an optimization problem. Unfortunately, this optimization can require many constraint function evaluations and would be computationally prohibitive in this algorithm. Therefore, the choice of an appropriate step length parameter at each iteration is based upon several other criteria: (1) maintaining closed loop stability, (2) maintaining open loop controller stability properties, and (3) improvement of the violated constraints. In order to maintain closed loop stability using discrete frequency data (as opposed to a mathematical model) the multivariable Nyquist criterion (ref. 6) is employed. Although it is not a reliable indicator of relative stability margins, it has proven effective in this algorithm for maintaining closed loop stability. Controller stability is achieved by simply monitoring the controller's poles. Although controller stability is not an absolute requirement, it is desirable in most applications, e.g., when loop failure is possible. As for the third criterion, the violated constraints are simply checked for improvements at each iteration. If they have improved, the parameter vector is updated and the step length is increased by a user defined factor for use at the next iteration. If not, the step length is reduced and the constraints are checked again. This process is repeated until improvements are registered or until the minimum step length allowed is reached. If the minimum step length is reached, then either a violated constraint has reached a local minimum or two gradients are in local opposition. In the case of a local minimum, the design can either be accepted or the constraint relaxed. The action to be taken if two gradients are opposed is now discussed.

In the case of two gradients in local opposition, the matrix J_k will be nearly rank

deficient and the correction vector d_k, although defined, will almost be orthogonal to all the gradient vectors. Hence, improving the constraints with an acceptable step length is highly unlikely. If one of the opposing gradients is not associated with the worst violation for that particular constraint, the problem can be circumvented by dropping that gradient from J_k at the current iteration. If, however, both gradients are associated with the worst violations of different constraints, then the constraints are not locally feasible and this technique will fail to improve the constraints. Hence, the algorithm is not guaranteed to satisfy all the design constraints, but it will improve the violated constraints until no further local improvement is possible. It is also important to note that even if the constraints are satisfied, they are only satisfied at the frequencies for which the design was performed. A flowchart of the complete algorithm is given in figure 1.

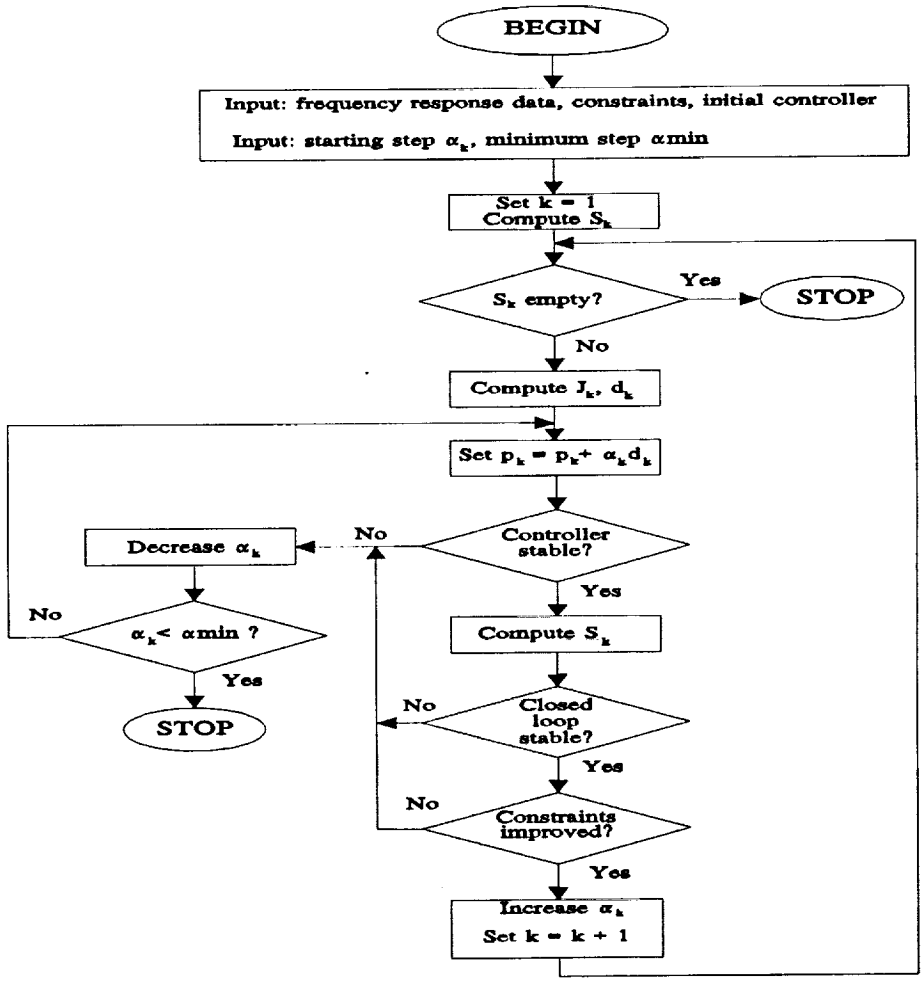

Figure 1: Algorithm Flowchart.

SELECTION OF A CONTROLLER REPRESENTATION

Two choices for a controller representation have been investigated. The most obvious choice is a state-space representation, i. e.,

$$K(e^{j\omega T}) = C(e^{j\omega T}I - A)^{-1}B + D, \tag{14}$$

where $K \in C^{q\times p}$, $A \in R^{n\times n}$, $B \in R^{n\times p}$, $C \in R^{q\times n}$, and $D \in R^{q\times p}$ for an n^{th}-order discrete-time control law with p inputs and q outputs. It can be shown that if $f(Q) \in R$, $Q = (A,B,C,D,\omega_i)$ (ω_i indicates a fixed frequency) is a function for which all the partials with respect to the entries of A, B, C, and D exist, then

$$\frac{\partial f}{\partial D}(Q) = Re\left[\left(\frac{\partial f}{\partial K}(Q)\right)^H\right]^T, \tag{15}$$

$$\frac{\partial f}{\partial C}(Q) = Re\left[\Phi B\left(\frac{\partial f}{\partial K}(Q)\right)^H\right]^T, \tag{16}$$

$$\frac{\partial f}{\partial B}(Q) = Re\left[\left(\frac{\partial f}{\partial K}(Q)\right)^H C\Phi\right]^T, \tag{17}$$

and

$$\frac{\partial f}{\partial A}(Q) = Re\left[\Phi B\left(\frac{\partial f}{\partial K}(Q)\right)^H C\Phi\right]^T, \tag{18}$$

where $\Phi = (e^{j\omega_i T}I - A)^{-1}$. An interesting property of this representation is that it is only unique up to a similarity transformation on (A,B,C,D). Hence, the possibility exists that by judicious selection of state coordinates the characteristics of the parameter space may be chosen to impact algorithm performance. This issue is a subject of current research.

As an alternative to a state-space representation, the so-called Gilbert realization,

$$K(e^{j\omega T}) = \sum_{i=1}^{n} \frac{x_i y_i^T}{e^{j\omega T} - \lambda_i} + D \tag{19}$$

where $\lambda_i \in C$, $x_i \in C^q$, and $y_i \in C^p$, has also been employed. An advantage of this representation is that for a given control law the number of parameters is considerably less than for a state-space representation. It has the disadvantage that the number of real poles and complex-conjugate pairs must remain the same throughout the iteration process.

ALGORITHM IMPLEMENTATION

At the present time the algorithm has been implemented in the FORTRAN programming language on a personal computer. Standard subroutine libraries in the public domain have been used extensively for singular value decompositions and eigen decompositions. The algorithm has also been implemented in the language of a popular matrix oriented software package.

CONTROLLER DESIGN FOR THE ACES STRUCTURE

A schematic of the NASA Marshall Space Flight Center ACES structure is shown in figure 2. The ACES structure is suitable for the study of line-of-sight (LOS) and vibration suppression control issues as pertaining to flexible aerospace structures. The primary element of the ACES structure, a spare Voyager magnetometer boom, is a lightly damped beam measuring approximately 45 feet in length and weighing about 5 pounds.

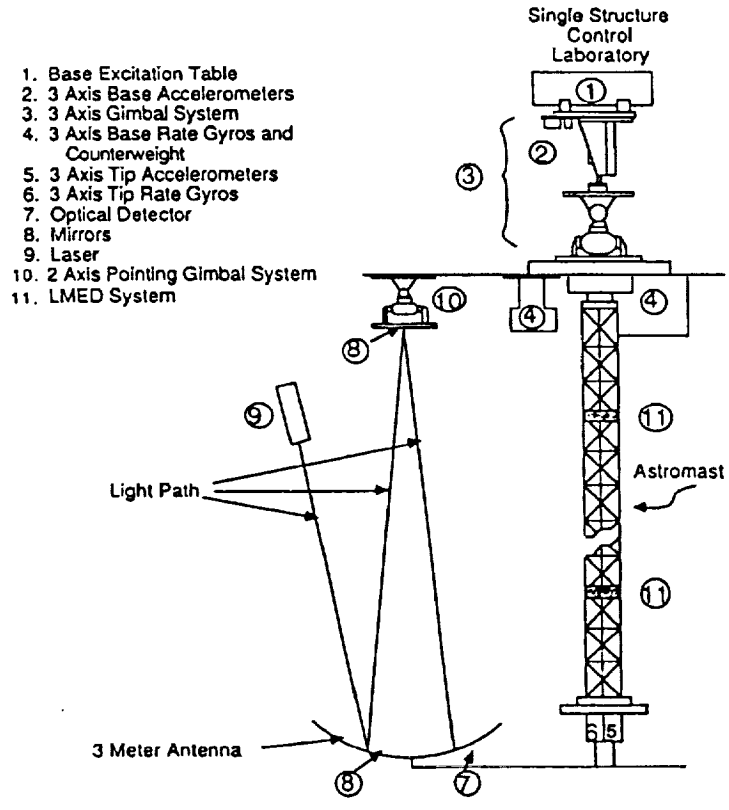

Figure 2: Schematic of the ACES Structure.

The goal of the control system design is to maintain the reflected laser beam in the center of the antenna (location of the detector) in the presence of disturbances at the base excitation table (BET). This is to be accomplished by use of the following actuators: Image Motion Compensation (IMC) gimbals (2-axes), Advanced Gimbal System (AGS) (3-axes), Linear Momentum Exchange Devices (LMED)'s (2 2-axes devices); and the sensors: base rate gyros (3-axes), tip accelerometers (3-axes), tip rate gyros (3-axes), LMED positions and accelerations (2-axes each) and the optical position detector (2-axes). As explained subsequently, our design only employed a subset of these sensors and actuators. The digital controller is to be implemented on the HP9000 computer located at the facility using the fixed sampling rate of 50 Hertz and a fixed, one sample period computational delay. The results of other controller designs for the ACES structure have been reported in the literature (ref. 7).

The experimental open loop frequency response from the y-axis IMC gimbal to the x-axis LOS error is shown in figure 3. The effect of the computational delay is quite apparent from analysis of the phase characteristic. The frequency responses of the other axes of the IMC-to-LOS are similar, although the cross-axis terms have less gain. The open loop frequency response from the y-axis AGS gimbal to the y-axis base gyro is shown in figure 4. This response reveals the numerous lightly damped modes of the structure. The frequency responses of other elements of the AGS-to-base gyros transfer matrix are similar. It is noted that the cross axis elements have considerable gains at some modal frequencies.

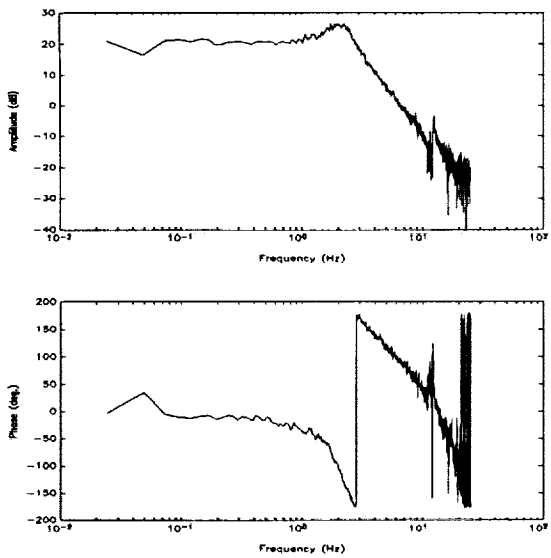

Figure 3: Experimental Frequency Response from y-axis IMC Gimbal to x-axis LOS Error.

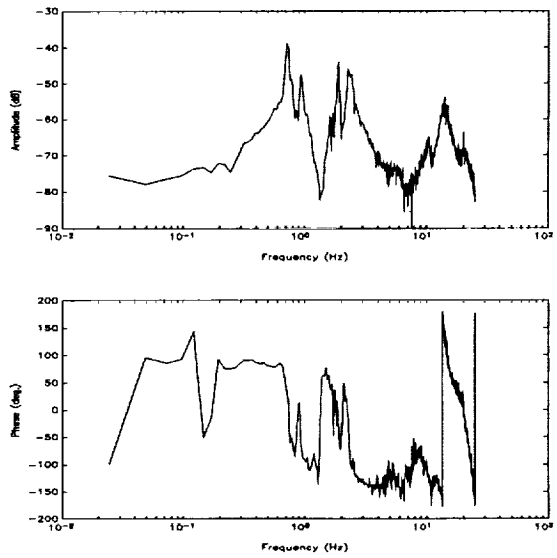

Figure 4: Experimental Frequency Response from y-axis AGS Gimbal to y-axis Base Gyro.

The basic design philosophy was to dampen the pendulum modes and the bending modes of the beam by using feedback from the base gyros to the AGS while using the IMC

gimbals with feedback from the detector to maintain the laser beam at the center of the detector. Due to sufficient decoupling, each two-input, two-output subsystem (AGS and IMC) was designed separately. One concern was the impact of disturbances that reach the IMC gimbals through the connecting arm that is attached to the base (as opposed to disturbances impacting the detector). Due to the inherently high optical gain from the IMC to the detector these disturbances can have a significant impact on the LOS error. To compensate for the effects of these disturbances it is not only necessary to maintain high loop gain over the frequency band of interest, but to also maintain high IMC controller gain as well. Analysis of figure 3 reveals that achieving high controller gain while also maintaining acceptable stability margins is difficult because of the combination of the high optical gain and the additional phase lag introduced by the computational delay. Fortunately, the impact of these disturbances can also be reduced by increasing the damping of the modes of the beam using the AGS; thereby reducing the motion of the base and the arm supporting the IMC gimbals.

The first step of the design procedure was the determination of a set of precise closed loop constraints such as those given in the first column of table 1. These constraints are primarily stability robustness constraints.

Table 1. Summary of Multivariable Design Constraint Values.

Constraint	Initial	Final
$\sigma_{\min}\left[I+GK(z)\right]_{IMC} > 0.5,\ f\in(0,25)$	0.2289	0.5090
$\sigma_{\min}\left[I+KG(z)\right]_{IMC} > 0.5,\ f\in(0,25)$	0.2276	0.5056
$\sigma_{\min}\left[I+(GK(z))^{-1}\right]_{IMC} > 0.6,\ f\in(0,25)$	0.2827	0.6072
$\sigma_{\min}\left[I+(KG(z))^{-1}\right]_{IMC} > 0.6,\ f\in(0,25)$	0.2805	0.6112
$\sigma_{\min}\left[I+GK(z)\right]_{IMC} > 18,\ f = 0.15$	10.002	14.100
$\sigma_{\min}\left[I+GK(z)\right]_{AGS} > 0.6,\ f\in(0,25)$	0.3649	0.5996
$\sigma_{\min}\left[I+KG(z)\right]_{AGS} > 0.6,\ f\in(0,25)$	0.3585	0.5988
$\sigma_{\min}\left[I+(GK(z))^{-1}\right]_{AGS} > 0.7,\ f\in(0,25)$	0.3600	0.6719
$\sigma_{\min}\left[I+(KG(z))^{-1}\right]_{AGS} > 0.7,\ f\in(0,25)$	0.3589	0.6712

IMC represents IMC subsystem
AGS represents AGS subsystem
G represents plant
K represents controller
$z = e^{j2\pi fT}$, $T = 0.02$ sec

C-2

The fifth constraint, a performance constraint, is included in particular to suppress the effect of a very lightly damped pendulum mode. Performance constraints were not included in the algorithm for the AGS subsystem, because after the design of the initial controllers, the primary concern for this subsystem was to guard against uncertainty. Analytical expressions for the gradients of these constraint functions were calculated using results from ref. 8 and equations 15-18.

Next, initial controllers were designed for the IMC-to-LOS and AGS-to-base gyro subsystems using graphical one-loop-at-a-time techniques with experimental frequency response data. Although the attempt was made to satisfy the constraints in designing the initial controllers, they were not satisfied as can be observed by comparing the first and second columns in table 1. The controller for each subsystem was 10^{th} order. It should be noted that recently developed high fidelity models are 60^{th} order for the AGS-to-base gyro loops alone (ref. 9) Design techniques such as LQG and H^{∞} would yield controllers of at least this order (not including weighting).

The multivariable design (i.e., taking cross-axis coupling within each subsystem into account) for each subsystem was then performed using only experimental data and the presented algorithm. The algorithm was started with the initial 10^{th} order controllers (using state-space representations) described above, with no restrictions other than stability placed on the structure of the controllers. To illustrate typical results from the algorithm, figure 5 and figure 6 show the experimental singular value frequency responses of $[I + GK]_{IMC}$ for the initial and final controllers, respectively. The final values of all the constraint functions are provided in the third column of table 1. The constraints for the AGS subsystem were not satisfied because the algorithm reached a point such that these constraint functions were in the condition of local opposition described previously.

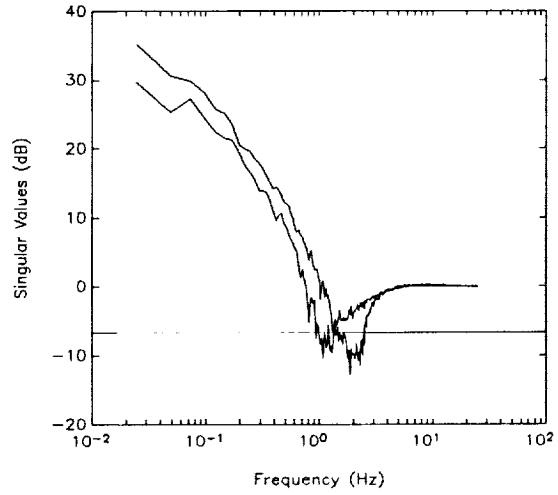

Figure 5: Initial Singular Value Frequency Response of $(I + GK)_{IMC}$.

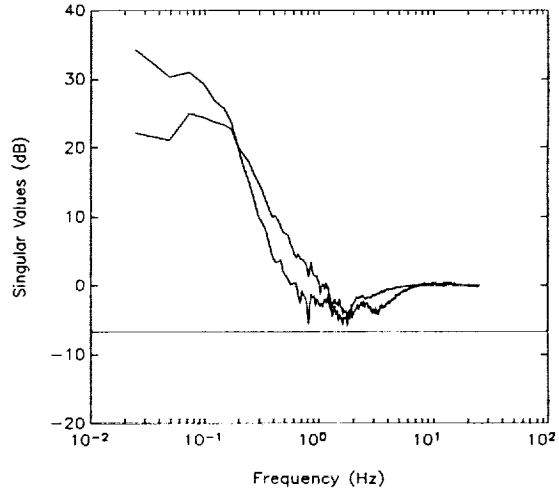

Figure 6: Final Singular Value Frequency Response of $(I + GK)_{IMC}$.

The resulting controller was implemented at the ACES facility. The open loop x-axis LOS error due to an x-axis BET disturbance (figure 7) intended to simulate the effect of spacecraft crew motion is shown in figure 8. The dominant behavior in the response is the lightly damped 0.15 Hz pendulum mode. After closing only the IMC-to-LOS loops the steady-state error and the impact of the pendulum mode were reduced as shown in figure 9. However, the first bending mode was still present. As shown in figure 10, closing the IMC-to-LOS *and* the AGS-to-base gyro loops further reduced the impact of the pendulum mode and almost eliminated the first bending mode. The y-axis LOS error was negligible.

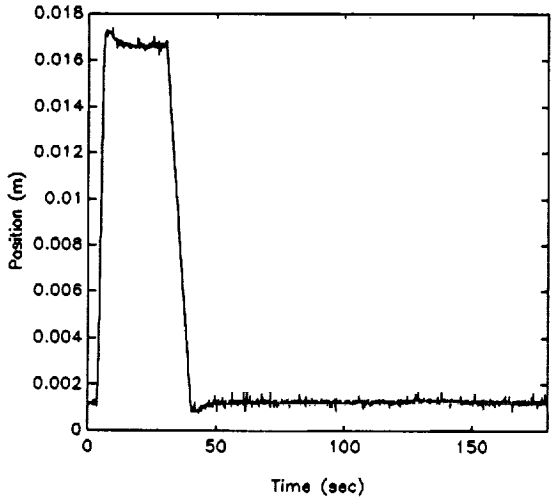

Figure 7: The x-axis BET Disturbance.

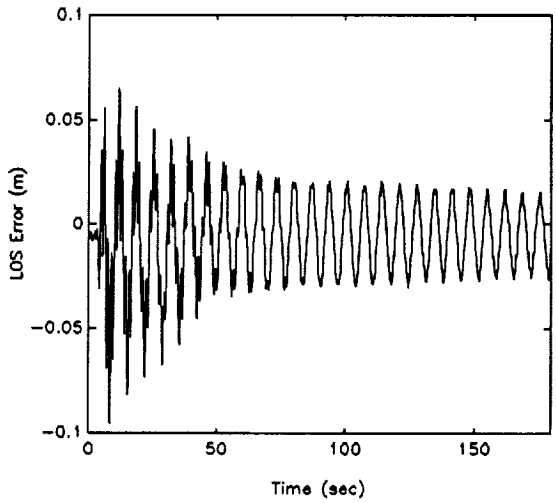

Figure 8: Experimental Open Loop x-axis LOS Error.

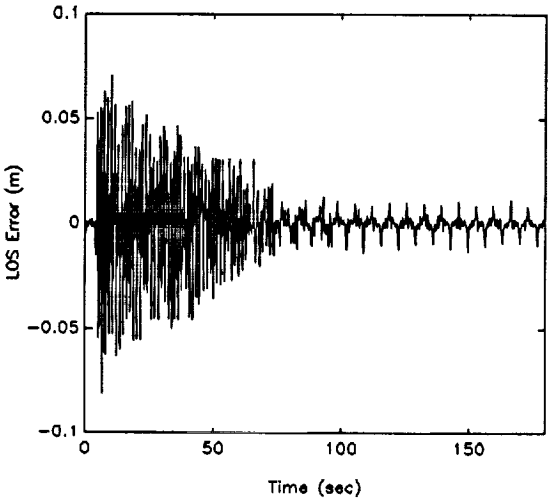

Figure 9: Experimental x-axis LOS Error with IMC Loops Closed.

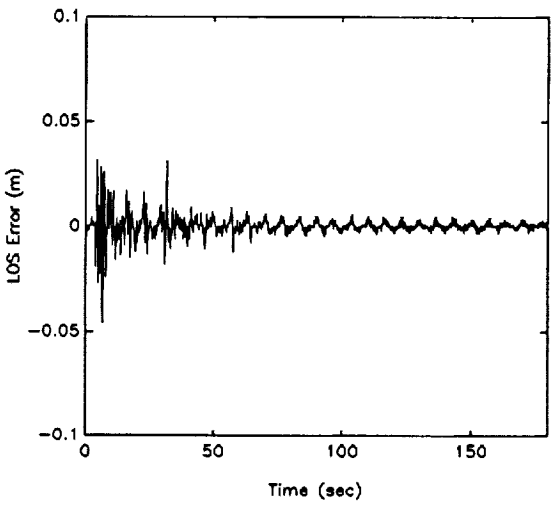

Figure 10: Experimental x-axis LOS Error with all Loops Closed.

To further indicate the effectiveness of the controller, x-y scatter plots of the LOS error are provided in figure 11 and figure 12, respectively.

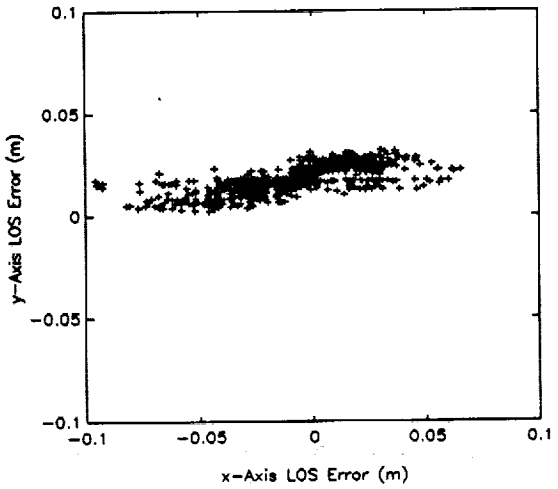

Figure 11: Experimental Open Loop x-y LOS Error.

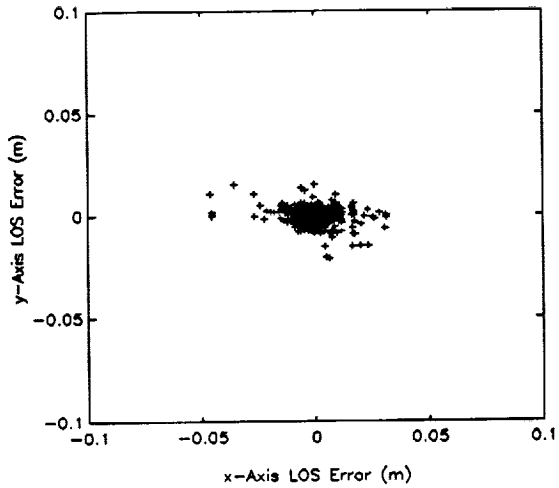

Figure 12: Experimental Closed Loop x-y LOS Error.

The same disturbance (figure 7) was applied to the y-axis of the BET. The open loop response of the x-y LOS error is shown in figure 13. The closed loop x-y LOS error is shown in figure 14.

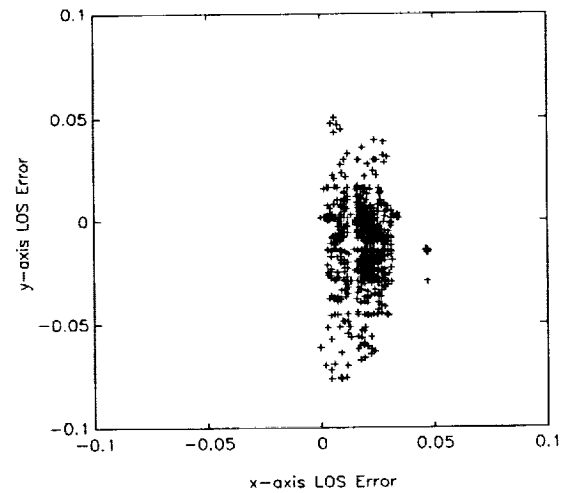

Figure 13: Experimental Open Loop x-y LOS Error.

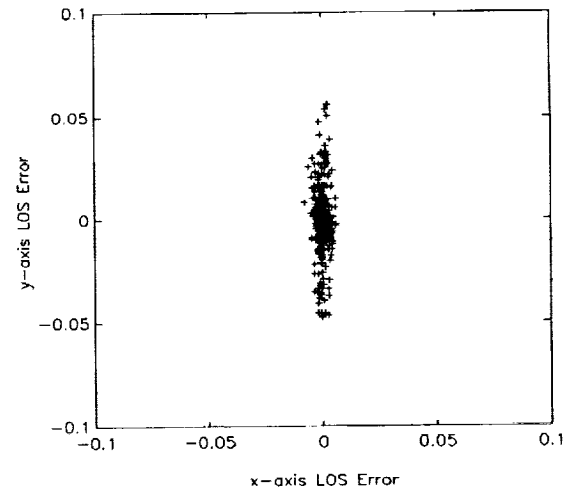

Figure 14: Experimental Closed Loop x-y LOS Error.

CONCLUSIONS

The application of an iterative numerical technique to controller design for a large space structure ground test facility has been presented, and the results appear to be very promising. The resulting controller was 20^{th} order which was low compared to controllers resulting from procedures such as H^{∞} or linear-quadratic-Gaussian. The presented technique has been shown to have the advantages that multiple closed loop design constraints can be simultaneously considered without the need for weighting schemes; the design engineer can have complete control over controller order and structure; the design can be performed with or without the use of a parametric plant model; and locally feasible, violated constraints can be improved at each iteration. Although the presented design example only involves constraints on matrix singular value frequency responses, there is no reason that the technique could not be applied to other constraints such as the shapes of individual elements of frequency response matrices and root-mean-square measures when such constraints are of interest.

ACKNOWLEDGMENTS

The authors would like to thank the NASA Marshall Space Flight Center and the Ohio Aerospace Institute for their support. Thanks is also due Dr. Jerrel Mitchell for his helpful comments.

REFERENCES

1. Boyd, Stephen P. and Barratt, Craig H., *Linear Controller Design: Limits of Performance*, Prentice-Hall, Englewood Cliffs, New Jersey, 1991.

2. Newsom, Jerry R. and Mukhopadhyay, V., "A Multiloop Robust Controller Design Study Using Singular Value Gradients," *Journal of Guidance, Control and Dynamics,* vol. 8, no. 4, pp. 514-519, July-August, 1985.

3. Mukhopadhyay, Vivek, "Digital Robust Control Law Synthesis Using Constrained Optimization," *Journal of Guidance, Control and Dynamics,* vol. 12, no. 2, pp. 175-181, March-April, 1989.

4. Golub, Gene H. and Van Loan, Charles F., *Matrix Computations,* 2 ed., The Johns Hopkins University Press, Baltimore, Maryland, 1989.

5. Mitchell, Jerrel R., *An Innovative Approach to Compensator Design,* Ph.D. dissertation, State College, Mississippi, May, 1972.

6. Postlewaite, I. and MacFarlane, A. G. J., *A Complex Variable Approach to the Analysis of Linear Multivariable Feedback Systems,* Springer-Verlag, New York, 1979.

7. Collins, E. G., Phillips, D. J., and Hyland, D. C., "Robust Decentralized Control Laws for the ACES Structure," *IEEE Control Systems Magazine*, vol. 11, no. 3, pp. 62-70, April, 1991.

8. Junkins, John L. and Kim, Youdan, "First and Second Order Sensitivity of the Singular Value Decomposition," The *Journal of the Astronautical Sciences*, vol. 38, no. 1, pp. 69-86, Jan.-March, 1990.

9. Medina, Enrique, *Multi-input, Multi-output System Identification from Frequency Response Samples with Applications to the Modeling of Large Space Structures*, M. S. Thesis, Ohio University, November, 1991.